Nanoscale

Accepted Manuscript

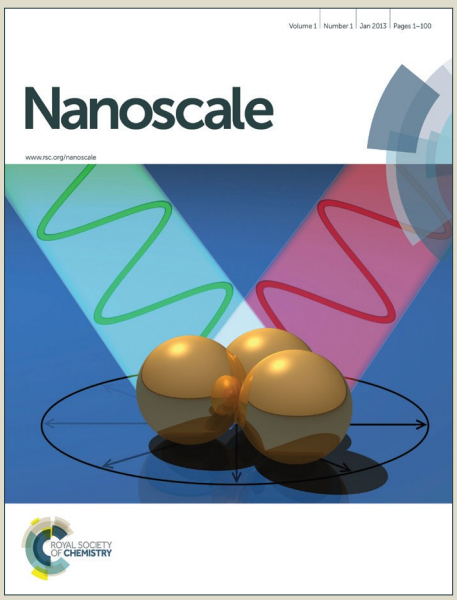

ROYAL SOCIETY OF CHEMISTRY

www.rsc.org/nanoscale

Nanoscale

FEATURE ARTICLE

Hairy cellulose nanocrystalloids: A novel class of nanocellulose

Theo G. M. van de Ven[a*] and Amir Sheikhi[a]

Received 00th January 20xx,
Accepted 00th January 20xx

DOI: 10.1039/x0xx00000x

www.rsc.org/

Nanomaterials have secured such a promising role in today's life that imagining the modern world without them is almost impossible. A large fraction of nanomaterials is synthesized from environmentally-dangerous elements such as heavy metals, which has posed serious side-effects to ecosystems. Despite numerous advantages of synthetic nanomaterials, issues such as renewability, sustainability, biocompatibility, and cost efficiency have drawn significant attention towards natural products such as cellulose-based nanomaterials. Within the past decade, nanocelluloses, most remarkably nanocrystalline cellulose (NCC) and nanofibrillated cellulose (NFC), have successfully been used for a wide spectrum of applications spanning from nanocomposites, packaging, and mechanical and rheological property modifications, to chemical catalysis and organic templating. Yet, there has been little effort to introduce fundamentally new polysaccharide-based nanomaterials. We have been able to develop the first kind of cellulose-based nanoparticles bearing both crystalline and amorphous regions. These nanoparticles comprise a crystalline body, similar to conventional NCC, which is attached to polymer chains protruding from both ends; therefore, called hairy cellulose nanocrystalloids (HCNC). In this article, we touch on the philosophy of synthesis, the striking superiority over existing nanocelluloses, and applications of this novel class of nanocelluloses. We hope that the emergence of hairy cellulose nanocrystalloids extends the frontiers of sustainable, green nanotechnology.

Introduction

Research on polysaccharide nanomaterials especially nanocrystals[1] and nanofibrils[2] is advancing with a fast pace. Among the polysaccharides, cellulose, the most abundant biopolymer in the world, has been the focus of sustainable nanotechnology due to its unique nanostructure.[3] Recent decades have witnessed remarkable interests for using nanocelluloses to develop new green materials such as composites[4,5] to replace synthetic materials, minimize the environmental side effects, and decrease production cost. The main focus of current nanocellulose research is on cellulosic bionanocomposites,[6] which have promisingly performed in a broad range of applications such as biomedicine,[7] food and packaging,[8,9] energy and electronics,[10–17] sensors and actuators,[18,19] and microfluidic devices[20] owing to their auspicious barrier and mechanical properties[21], low surface roughness[22], abundance and biodegradability[23], and ease of adhesion[24] and processing. Despite significant efforts to design, synthesize, and characterize nanocellulose-based composites, little effort is devoted to developing new nanocellulosic building blocks.

Compared to most other nanomaterials, nanocelluloses can be produced in large quantities[25] through chemical and/or mechanical treatments at moderate cost. By 2020, the gross domestic product (GPD) of nanocelluloses is estimated to be $600 billion in the world including $200 billion in the United States of America alone.[26] Most nanocelluloses are prepared from cellulose[27] and lignocellulosic[28] fibers, but can also be produced from algae and bacteria.[29] Nanocellulose is a renewable material, it is biodegradable and has exceptional strength properties,[27] which makes it superior compared to other carbohydrate-based nanomaterials. For example, starch, one of the most abundant natural polymer, can also be treated mechanically (e.g., microfluidization) or chemically (e.g., hydrolysis) to produce amorphous or crystalline nanoparticles, respectively.[30] The yield of chemical methods is often significantly lower than mechanical treatments and poor mechanical endurance and strong water affinity of starch films have led material scientists towards preparing cellulose-based starch nanocomposites.[31]

Nanocellulose comes in two major forms: cellulose nanofibrils (CNF) and nanocrystalline cellulose (NCC) (also referred to as cellulose nanocrystals (CNC) or cellulose nanowhiskers). CNFs are long slender rod-like particles, typically with a width of about *O*(10) nm and a length up to several microns.[32] They can be produced from cellulose fibers by an energy intensive mechanical treatment,[33] but usually are pretreated first to reduce the energy consumption. Typical pretreatments are enzymatic or chemical pretreatments.[34] The most common pretreatment is a TEMPO (2,2,6,6-tetramethylpiperidine-1-oxyl)-mediated oxidation of the cellulose fibers.[35] TEMPO is a catalyst which oxidizes the hydroxyl groups on the C6 position of the glucose units and converts them to carboxyl groups.[36,37] Typically, the charge density of such TEMPO-oxidized cellulose

[a] *Department of Chemistry, Pulp and Paper Research Centre, and Centre for Self-Assembled Chemical Structures, McGill University, 3420 University Street, Montreal, Quebec H3A 2A7, Canada. E-mails: theo.vandeven@mcgill.ca; amir.sheikhi@mail.mcgill.ca; Fax: +514-398-8254; Tel: +514-398-6177*

nanofibrils (TOCF) is up to 1.6 meq g^{-1}. For a more in-depth study, readers are referred to the literature.[38–40]

CNF is the major building block of wood fibers and, for delignified fibers, the wood cell wall consist mainly of bundles of CNF.[41] CNF consist of alternating crystalline and amorphous cellulose regions (Fig. 1). NCC, often produced from removing all amorphous regions of fibers, has a similar diameter to CNF but is typically 100-200 nm long.[42] The most common way of producing NCC is by acid hydrolysis using sulphuric acid, in which process the amorphous regions react referentially with the acid, resulting in the breakdown of the amorphous regions in sugars and oligosaccharides. What remains are the crystalline regions, i.e., NCC. Because of using sulphuric acid, NCC is sulfonated, typically with a charge density of about 0.2 meq g^{-1}, which can be further oxidized by TEMPO, similar to CNF.[43]

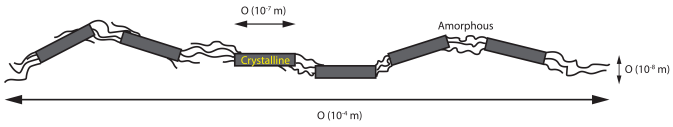

Fig.1 Schematic of cellulose nanofibrils (CNF), the major building blocks of cellulose fibers, consisting of alternating crystalline and amorphous regions.[44]

The length and width of the crystalline and amorphous cellulose regions depend on the source of cellulose.[42,45] In plants and trees, they determine to a large extent the strength, flexibility, and water absorbency. In bacterial cellulose, crystalline regions dominate and make up most of the CNF. Usually long crystalline regions have a larger diameter than less crystalline CNF.

An important property of CNF is that the crystalline regions are twisted, and, thus NCC has a twist as well, i.e., it is chiral.[46] As a result, suspensions of NCC are cholesteric (chiral nematic) and present beautiful iridescent colors. Usually, this twist is thought of as a (right-handed) twisting of a rod. Recently, quantum mechanical calculations on NCC crystals have shown that each cellulose chain in the crystal is twisted, but some are twisted right handed and others left handed.[47] The combined effect is a right handed twist. Thus, NCC particles are not perfect crystals, and we refer to them instead as crystalloids. Quantum calculations also show that the twist changes sign for thinner crystalloids,[47] an effect also observed experimentally in our lab (to be submitted).

Hairy cellulose nanocrystalloids

As discussed, (conventional) NCC is produced by acid hydrolysis of the amorphous regions in cellulose fibers. The preferential reaction of chemicals with the amorphous regions is not restricted to acid, but applies to almost all chemical reactions with cellulose fibers. Amorphous regions are more kinetically accessible, thus, most chemical modifications of cellulose fibers result in a preferential modification of the amorphous regions. Cellulose is not soluble in water; however, it is possible to modify the amorphous regions in such a way that favors their dissolution. This would happen if all the chain ends of the cellulose chains, making up a cellulose nanofibril, were located in the amorphous regions. If the chain ends are distributed among the crystalline and amorphous regions, it is also necessary to cleave the chains in the amorphous regions to favor the hydrophilically modified amorphous regions to go in solution. This suggests a novel way to make nanocelluloses: we can solubilise the amorphous regions, while, at the same time, cleaving a sufficient number of cellulose chains. In such a scenario, the nanofibers shall fall apart in the crystalline regions, while still bearing the amorphous regions attached to their ends. We have shown that this is indeed possible. A reaction which converts cellulose to a water-soluble cellulose derivative is the reaction with periodate (Fig. 2).

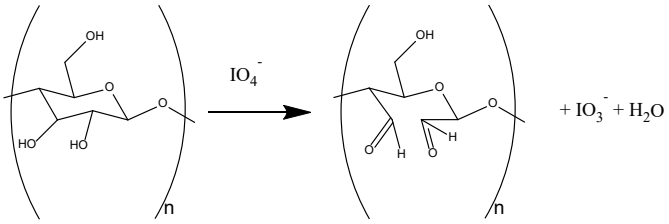

Fig. 2 Reaction of periodate with cellulose yields dialdehyde cellulose DAC, when going to full conversion. For partial conversion, it results in dialdehyde modified cellulose (DAMC), a copolymer of glucose and dialdehyde glucose.[48–51]

Periodate stereospecifically converts the C2-C3 hydroxyl groups of the glucose units into aldehydes, while simultaneously breaking the C2-C3 bond.[49] Cellulose dialdehyde is soluble in water at room temperature (but requires heating to initiate the dissolution); thus, the reaction of periodate with cellulose results in the solubilisation of the amorphous regions. At the same time, the dialdehyde-modified cellulose chains can be cleaved (Fig. 3).

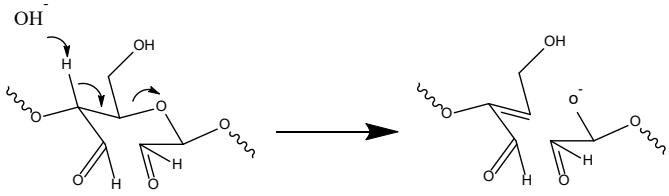

Fig. 3 Chain cleavage of DAMC in a slightly basic[52] medium. In an acidic environment, the β-linkage is attacked by H^+, resulting in the cleavage of glycoside bonds.[53]

Accordingly, it is anticipated that when periodate-oxidized fibers are heated, they fall apart in nanocrystalline cellulose with the amorphous regions still attached to both ends (Fig. 4). This is indeed what happens.

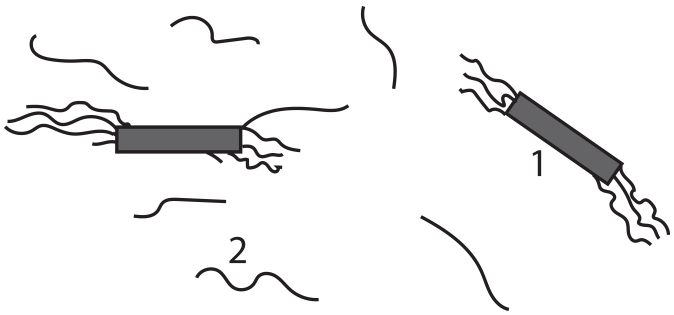

Fig. 4 Reaction products of periodate-oxidized fibers: (1) NCC with solubilised amorphous regions at each end and (2) dissolved solubilised chemically modified cellulose chains. Note that in conventional NCC, the protruding chains are absent, and the amorphous regions are converted to sugars and oligosaccharides.[54,55]

The kinetics of the periodate reaction with fibers can be accelerated by adding an inert salt. For the reaction to occur, the negatively charged periodate ions have to penetrate the negatively charged pores of the fiber wall. Because of a Donnan equilibrium,[56] the concentration of periodate in the pores is much lower than in the bulk. By adding salt, the the Donnan equilibrium is shifted, increasing the concentration of periodate in the pores, thus increasing the reaction rate.

The advantage of the periodate reaction with cellulose fibers is the possibility of maintaining the fibers intact prior to heating. Thus, all the chemicals can be readily separated and the fibers can be washed before making them fall apart in nanocelluloses (by heating). The produced iodate (see Fig. 2) can be converted back to periodate in a reaction with hypochlorite under alkaline conditions (Fig. 5).[57] Thus, the cost of the periodate reaction is mainly the chemical cost of (non-expensive) hypochlorite, the expenses of running a recovery cycle, and the cost of the make-up periodate, since the recovery cycle is unlike to operate at 100% efficiency.

$$ClO^- + IO_3^- \rightarrow Cl^- + IO_4^-$$

Fig. 5 Recovery of periodate through the reaction of iodate with hypochlorite in a basic medium.[57]

We refer to the nanocellulose produced by the periodate reaction followed by heating at 80°C as sterically stabilized nanocrystalline cellulose (SNCC),[54] since the dialdehyde chains (or, more precisely, the dialdehyde modified cellulose chains, DAMC) protruding from both ends, provide steric stability. SNCC particles carry no charge. Owing to the high reactivity of aldehydes groups, SNCC or DAMC may act as precious intermediates, which can be functionalized with other chemical groups. For instance, a chlorite oxidation of periodate-oxidized fibers results in carboxyl groups, whereas a Schiff base reaction with a molecule bearing a primary amine (R-NH_2) results in the attachment of a group R of our choice. This way, we have produced cationic NCC (CNCC)[58] in which R carries a quaternary ammonium group. Furthermore, the nanocelluloses produced from the chlorite oxidation bear dicarboxylated cellulose chains protruding from both ends. These charged chains provide electrostatic and steric (electrosteric) stability, thus we name these nanoparticles electrosterically stabilized NCC (ENCC). Note that CNCC is also electrosterically stabilized.

To solubilise the amorphous regions by introducing charge, it is necessary to attach a sufficient number of charge groups to the amorphous regions. For this purpose, a minimum of 3 meq g^{-1} is required. In case of lower charge densities, mechanical energy (e.g., vigorous stirring) is required to convert the fibers to nanocelluloses. Fundamentally, the lower the charge, the more energy is required to disintegrate the fibers. The amorphous regions can also be solubilised with less than 3 meq g^{-1}; however, the fiber disintegration has to be carried out at a high temperature, as the solubility increases with temperature.

In this article, we review the synthesis of SNCC, ENCC, and CNCC in detail, briefly discuss their characteristics and properties, and finally touch on their potential applications. We refer to this novel class of nanocelluloses bearing both amorphous and crystalline regions with tuneable charge as hairy cellulose nanocrystalloids (HCNC), or hairy nanocrystalline cellulose (HNCC).

Synthesis of hairy cellulose nanocrystalloids

Synthesis of SNCC

Softwood kraft pulp (1 g) is allowed to soak in water for at least one day to obtain swollen fibers and enhance the disintegration followed by dispersion by rigorous mixing. The disintegrated wet pulp is vacuum filtered and reacted with an aqueous solution of 0.66 g $NaIO_4$ and 3.87 g NaCl including total water volume V ≈ 200 mL.[54] Note that the moisture of wet pulp must be considered in preparing the final reaction solution. To prevent the deactivation of periodate, the reaction beaker is wrapped and covered with several layers of aluminum foil, and the oxidation reaction is allowed to proceed for 96 h at ambient temperature while the mixture is stirred at 105 rpm. To stop the reaction, ethylene glycol is added to the reaction suspension, which quenches the unreacted periodate. This is followed by removing the chemicals from the fibers by thorough rinses of deionized (DI) water, filtration, and resuspension in 100 mL DI water (including the wet pulp water content). The suspension is heated at 80°C in a round bottom flask while stirring gently for 6 h followed by cooling to room temperature and 10 min centrifugation at 15000 rpm to separate any non-fibrillated fibers (if present).

At this stage, a transparent suspension, containing SNCC and dissolved dialdehyde modified cellulose (DAMC, a copolymer of glucose and dialdehyde glucose) is obtained. To obtain SNCC, it is necessary to separate it from DAMC dissolved in the solution. This can be achieved by adding a cosolvent, which is a poor

solvent for DAMC, such as propanol.[54] Figure 6 shows an example of the separation of SNCC and DAMC.

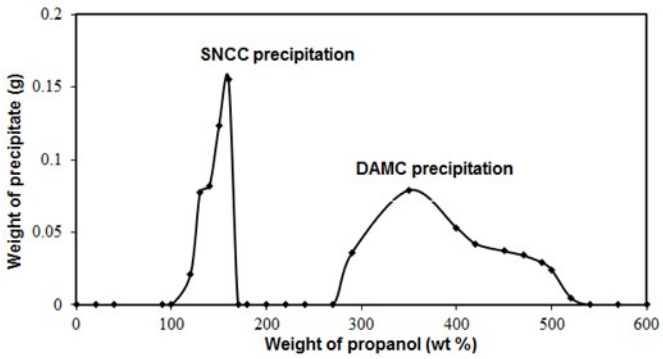

Fig. 6 Separation of SNCC from DAMC by cosolvent (propanol) addition.[54] With permission of Springer.

By adding propanol, SNCC precipitates out first, followed by the precipitation of DAMC. According to the theory of sterically stabilized colloids,[59] flocculation of colloids starts to occur when the Flory-Huggins polymer-solvent interaction parameter χ equals 0.5 (θ-solvent) or exceeds it.[60] For polymers to phase separate out of a solution, the χ-parameter must be larger than a critical value χ_c, which is larger than 0.5 for polymers of finite length.[61] When adding propanol, the χ-parameter increases, and one does expect SNCC to precipitate out first, followed by DAMC. This is in agreement with our observations.[54]

After the SNCC particles precipitated, they can be washed and redispersed in water. This results in a stable dispersion of SNCC particles without aggregation. Figure 7 shows an AFM image of SNCC (left) and, for comparison, an AFM image of conventional NCC, suggesting that SNCC has similar dimensions as NCC. The amorphous chains cannot be seen in AFM, but their existence can be inferred from the dynamic light scattering (DLS) experiments (Fig. 8).

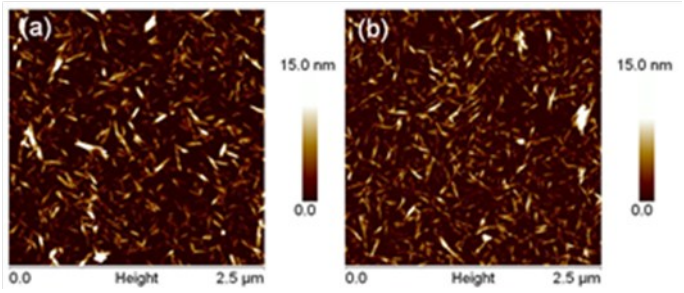

Fig. 7 Atomic force microscopy (AFM) image of (a) SNCC and (b) NCC attests to identical crystalline parts.[54] With permission of Springer.

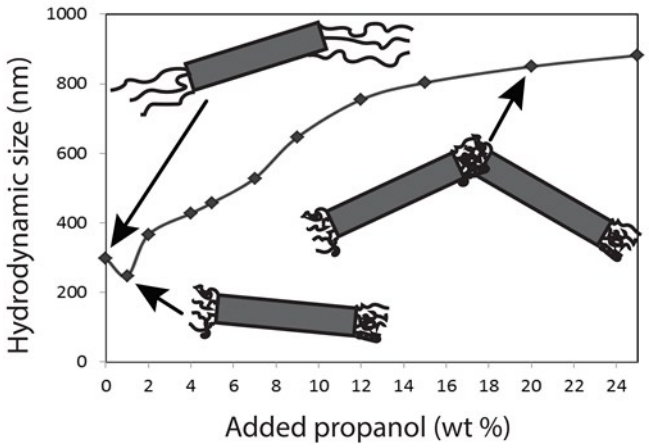

Fig. 8 Hydrodynamic size of SNCC versus added cosolvent acquired by dynamic light scattering (DLS). Steric stability of SNCC is reduced by adding propanol, resulting in the contraction of protruding chains, followed by aggregation.[54] With permission of Springer.

Figure 8[54] shows that, in pure water (in the absence of propanol), SNCC particles have an equivalent hydrodynamic spherical diameter of about 300 nm. This is larger than conventional NCC, presumably because of the protruding chains. For 1 wt % added propanol, the size decreases to about 240 nm due to the contraction of the chains in the poor solvent. At higher propanol/water ratios, the size increases due to the loss of steric stability, resulting in the formation of small aggregates. At even larger propanol additions, the aggregates become sufficiently large to sediment out of solution. This behavior is typical of sterically stabilized colloids.

The size of the SNCC particles can be controlled by the reaction condition. Increasing the periodate oxidation reaction time results in SNCC with a higher content of aldehydes groups.[54] The resulting particles have shorter crystalline regions, with insignificant change in their diameter. This implies that the periodate reaction in the later stages of the reaction (after most of the amorphous regions are oxidized) occurs mainly at the boundary of the amorphous and crystalline regions, creating a reaction fronts which advance towards the centre of the crystalline regions, thus shortening them.[55] The yield of SNCC production is typically about 50%. The remaining consists of solubilised DAMC chains.

Synthesis of ENCC

In principle, ENCC may be produced by, for example, a chlorite oxidation of SNCC; however, it is simpler to perform the reaction on the cellulose fibers after the completion of periodate reaction. In this way, the heating step can be eliminated, because the introduction of carboxyl groups in the amorphous regions of the fibers results in their solubilisation. Thus, the first step in the recipe to produce ENCC is the same as for making SNCC (i.e., periodate oxidation). After the

periodate reaction is quenched and the fibers are washed, the chlorite oxidation is performed (Fig. 9) during which the fibers fall apart in ENCC and dicarboxylated cellulose (DCC) after a sufficient number of carboxyl groups are introduced (≥ 3 mmol g^{-1}).[62]

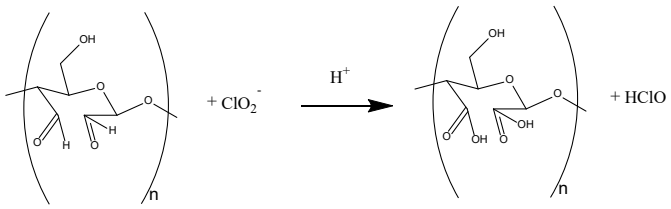

Fig. 9 Reaction of dialdehyde modified cellulose fibers with chlorite.[63,64] Hydrogen peroxide is also added to the reaction to convert HClO to HCl, O_2, and H_2O and minimize its reverse effect on the oxidation of DAMC.[65]

A standard recipe for a chlorite oxidation is as follows:[66,67] the dialdehyde modified pulp (1 g, dry basis) is suspended in water containing 3.56 g $NaClO_2$ and 14.6 g NaCl to achieve 250 mL solution including the wet pulp moisture content, followed by the addition of 3.3 g H_2O_2 while stirring at 105 rpm and ambient temperature. Upon the start of reaction, pH decreases, which should be maintained at 5 by continuous NaOH (0.5 M) addition. After 24 h, a translucent suspension is obtained. The disappearance of pulp indicates the breakdown of cellulose fibers. The mixture is centrifuged to separate the small amount of remaining large fibers, and gradual coprecipitation with ethanol is conducted to precipitate ENCC followed by by the centrifugation to separate ENCC from solubilised dicarboxylated cellulose (DCC) chains. DCC is the second product, which is isolated by an ethanol-mediated coprecipitation, similar to ENCC. The yield of ENCC production is typically about 50%, and the remaining is the DCC chains. A thorough hands-on SNCC/DAC and ENCC/DCC syntheses procedure is available as a visual experiment paper.[68]

Besides the chlorite oxidation, it is also possible to introduce part of the charges by a TEMPO-mediated oxidation of fibers.[67] An AFM image of ENCC is shown in Figure 10 (left). The amorphous protruding chains cannot be captured by the AFM. To investigate the role of protruding chains in charge regulation, ENCC is hydrolysed by a strong acid (e.g., HCl) treatment to produce hydrolysed ENCC (H-ENCC) (Fig. 10 (right)). H-ENCC has the same sizes as ENCC bearing a reduced charge, since most of the charge groups are located in the protruding chains, which have been chopped off.

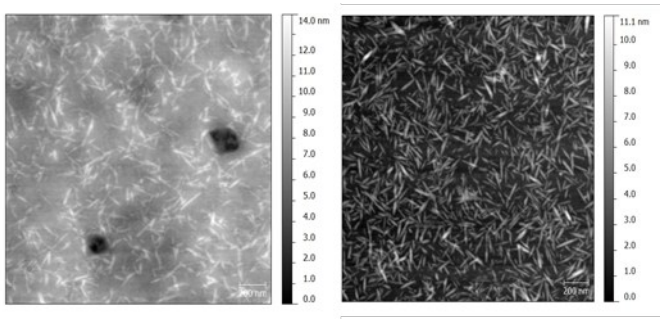

Fig. 10 Atomic force microscopy (AFM) image of ENCC (with a charge density of 6.6 meq g^{-1}) (left) and hydrolyzed ENCC (with a charge density of 1.4 meq g^{-1}) (right). Note that a charge density of 6 meq g^{-1} corresponds to a degree of substitution DS = 1. Both ENCC and H-ENCC are about 100-200 nm long and have a diameter of about 10 nm.[66] With permission of Springer.

Synthesis of CNCC

Cationic NCC with protruding amorphous regions (CNCC) can be produced in a number of ways. SNCC can be used as a starting material to react with R-NH_2 through a Schiff base reaction in which R contains a cationic group, or ENCC can be transformed into CNCC by a bioconjugation reaction[69] in which the carboxyl groups of ENCC are reacted with R-NH_2 on ENCC, using a suitable activator (e.g., 1-ethyl-3-(3-dimethylaminopropyl)carbodiimide hydrochloride, EDC); however, the simplest method is to perform a reaction on the dialdehyde modified cellulose fibers (DAMC), allowing the aldehydes groups to react with R-NH_2 (Fig. 11). If the charge groups are introduced at a density less than 3 mmol g^{-1}, the fibers will remain intact, and all chemicals can be readily removed and the fibers thoroughly washed. Further heating of the fibers solubilises the amorphous regions. For a charge content of ≈ 1.7 meq g^{-1}, the temperature needs to be increased to 60°C to solubilise the amorphous regions and produce CNCC.[58]

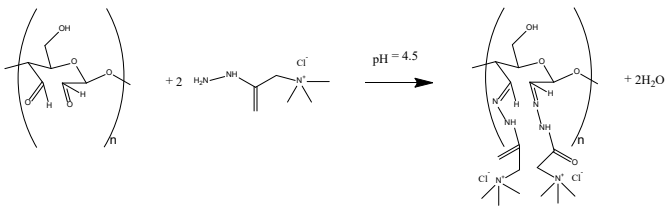

Fig. 11 Schiff base reaction between aldehydes groups on modified cellulose fibers with Girard's reagent T ((2-hydrazinyl-2-oxoethyl)-trimethylazanium chloride). Note that it is difficult to attach the second quaternary ammonium group to the same glucose unit due to steric hindrance and electrostatic repulsion.[58]

A typical recipe for producing CNCC is the following: DAMC (never-dried, containing 0.5 g dry DAMC) is added to a solution of Girard's reagent T (0.5 g) and NaCl (1.2 g) in 40 g water followed by adjusting the pH to 4.5 by HCl addition and stirring for 24 h in a 100 mL beaker at room temperature. The converted DAMC to cationic DAMC

(CDAMC) is washed thoroughly with water and filtered, followed by dispersion in water and heating at 60°C for 30 min to obtain a clear suspension. The suspension is centrifuged at 8000 rpm for 10 minutes and a negligible amount of non-fibrillated CDAMC fibers is removed by decantation. CNCC is obtained by propanol-mediated coprecipitation followed by centrifugation, which can be dialyzed and redispersed in water. Figure 12 shows the AFM and TEM images of CNCC.

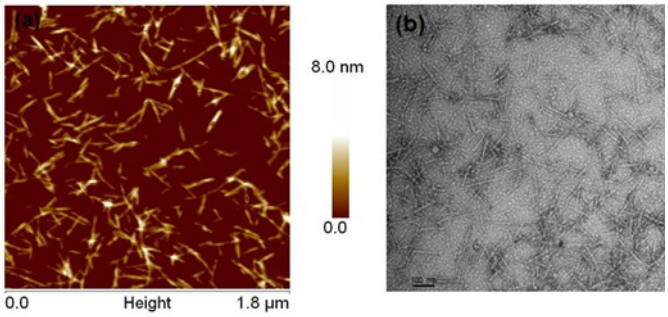

Fig. 12. AFM (left) and TEM (right) images of CNCC. Charge density ≈ 1.7 meq g^{-1}.[58] With permission of Springer.

The yield of CNCC is typically 50%. The remaining consists of dissolved chemically modified cellulose chains containing quaternary amine groups, QAMC (quaternary amine modified cellulose). More details about the synthesis of hairy nanoparticles can be found in.[58]

Morphology of hairy cellulose nanocrystalloids

AFM and TEM images show that SNCC, ENCC, and CNCC particles have dimensions similar to conventional NCC, i.e., length ≈ 100-200 nm and width ≈ 5-10 nm; however, the protruding chains are not detectable with these techniques. Their presence can be confirmed by other techniques, such as dynamic light scattering (DLS) or acoustic attenuation.[70] An example of this is already demonstrated in Fig. 8, where the chain size reduces by introducing the particles to a poor solvent (water-propanol mixture). Similarly, the size of dicarboxylated chains on ENCC can be reduced by adding salt, which screens the electrostatic repulsion between the charge groups. A similar phenomenon applies to CNCC. An example is presented in Fig. 13 in which the apparent size of ENCC (obtained by acoustic attenuation) is plotted versus salt (KCl) concentration.[70]

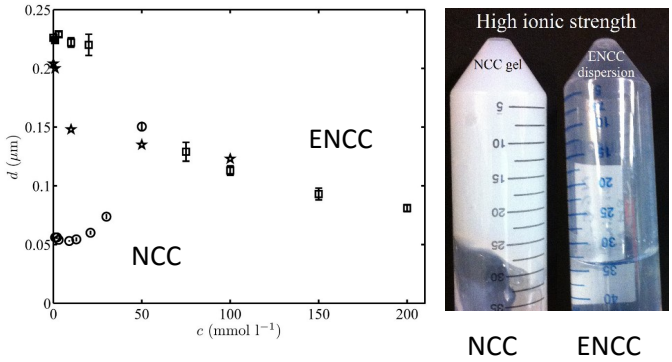

Fig. 13 (left) Size of ENCC particles obtained by acoustic attenuation (squares) or DLS (stars) as a function of salt (KCl) concentration. For comparison, results for conventional NCC (circles) are included. (right) NCC aggregates at a salt concentration as low as 40 mM and forms a gel, whereas ENCC remains as a stable colloidal suspension even at as high as 200 mM KCl.[71] Reprinted from J. Colloid Interface Sci., 432, S. Safari, A. Sheikhi, and T. G. M. van de Ven, Electroacoustic characterization of conventional and electrosterically stabilized nanocrystalline celluloses, 151-157, Copyright (2014), with permission from Elsevier.

It can be observed in Fig. 12 that ENCC size is largest in distilled water (≈ 220 nm) and decreases to about 100 nm at a high salt concentration, because the electrostatic screening results in the chain collapse. In comparison, the size of conventional NCC increases because of aggregation. ENCC is extremely stable and does not aggregate under the experimental conditions of Fig. 13. Similar results have been obtained with DLS.

The results from DLS and acoustic attenuation prove the existence of protruding chains; however, they do not confirm that the chains protrude from both ends of the crystalline body. Strong evidence that the chains are located at the end arises from the crosslinking of hydrolysed NECC (H-ENCC). In H-ENCC, most of the chains have been cleaved through acid hydrolysis, therefore it can be assumed that H-NCCs consist of NCC particles bearing negatively charged carboxyl groups at both ends. Crosslinking the carboxyl groups through bioconjugation with a diamine or azide-alkyne cycloaddition of two separately functionalized H-ENCC batches results in long rod-like particles, which attests to the end-to-end particle linkage (Fig. 14). This confirms that after the hydrolysis, the remaining charge groups are mainly located at the end of the particles, which implies that prior to the hydrolysis, the chains were protruding from both ends.[72]

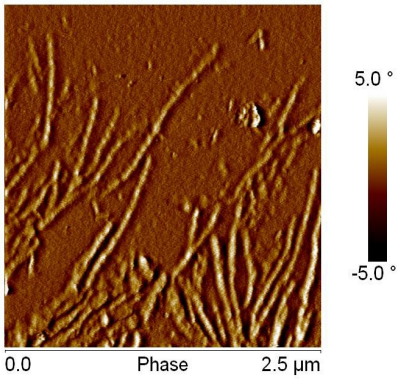

Fig. 14 AFM image of long rods obtained from chemically end-to-end assembly of hydrolysed ENCC. Through the ADH and EDC mediated bioconjugation, hydrolysed ENCC-NH2 and hydrolysed ENCC self-assembled. This attests to the existence of the functional groups (protruding hydrolysed DCC chains) on both ends of H-ENCC.[72]

Determination of functional groups content

Determination of aldehyde groups

The hydroxylamine hydrochloride method[73] can be used to determine the aldehyde content of oxidized cellulose by converting the dialdehyde cellulose to oximes. Briefly, a desired amount of dialdehyde cellulose is suspended in water (pH = 3.5, adjusted by HCl) followed by the addition of 10 mL hydroxylamine hydrochloride solution (5 wt %). The pH is maintained at 3.5 by NaOH addition (0.1 M) until a steady pH is achieved. The consumed NaOH is a direct indication of the aldehyde content. To express the aldehyde content in mol g^{-1}, the weight of each sample needs to be measured after complete drying. Complete conversion of cellulose to dialdehyde cellulose (DS = 2) corresponds to about 12 mmol g^{-1}. An alternative method of determining the aldehydes content is to convert the aldehyde groups to carboxyl groups and perform a conductometric titration (next section).

Determination of carboxyl groups

The carboxyl group content can be determined by a conductometric titration.[74] Typically, 20 mg ENCC (dry mass, can also be added from the aqueous ENCC suspension knowing its accurate concentration) and 2 mL NaCl solution (20 mM) are added to 140 mL milli-Q water, followed by stirring. HCl (0.1 M) is added to the well dispersed suspension to adjust the pH to 3. Gradually, a NaOH solution (10 mM) is added at 0.1 mL min^{-1} to the dispersion to achieve pH = 11. The length of the weak acid curve on the titration graph yields the carboxyl content (Fig. 15).

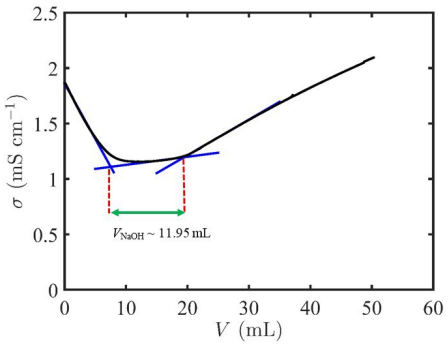

Fig. 15 An example of the conductometric titration of ENCC. Conductivity versus added NaOH (10 mM) is shown for 20 mg ENCC bearing 5.98 mmol g^{-1} carboxylic acid.[68]

Determination of quaternary amine content

The content of cationic groups (such as trimethylazanium chloride) can be determined by a conductometric titration using a silver nitrate solution. In this method, the concentration of counterions (e.g., chloride) is measured. Typically, $AgNO_3$ (10 mM) is used to titrate a 100 mL CNCC suspension at a rate of approximately 0.1 mL per 50 seconds. The conductance starts decreasing as soon as AgCl starts precipitating.[58] The titration end point is achieved when all the chloride ions precipitate as AgCl. As soon as the endpoint is achieved, the conductivity increases. An example of a conductometric titration of CNCC with $AgNO_3$ is presented in Fig. 16.

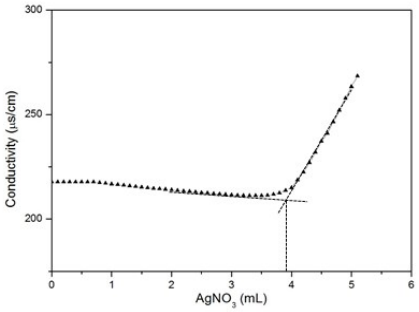

Fig. 16 Conductivity versus added $AgNO_3$ volume: conductometric titration curve for 120 mL CNCC bearing 1.68 mmol g^{-1} reacted with 10 mM $AgNO_3$. The CNCC was prepared from dialdehyde cellulose with 2.8 mmo g^{-1} aldehyde content.[58] With permission of Springer.

Other characterization techniques

Besides the microscopic techniques (TEM and AFM) and the particle size measurement techniques (DLS and acoustic attenuation) already mentioned, hairy nanocellulose can be characterized by a number of standard techniques, such as scanning electron microscope (SEM), Fourier transform infrared spectroscopy (FTIR), X-ray powder diffraction (XRD), X-ray photoelectron spectroscopy (XPS), solid state ^{13}C nuclear magnetic resonance (NMR), ultraviolet-visible (UV-vis) spectroscopy, electrophoretic light scattering (ELS) and electro-acoustic spectroscopy (EAS), thermogravimetric analysis (TGA), tensile strength and Young's modulus measurements, contact angle measurements, barrier properties evaluation for oxygen and water vapor, etc. Details can be found in our original articles on ENCC,[66,67,70,71] SNCC,[54,55] and CNCC.[58]

Evidences for the existence of protruding nanocellulose chains on HCNC

Evidence of protruding chains

Here, we summarize direct and indirect evidences supporting the existence of protruding nanocellulose chains. (i) The hydrodynamic size of ENCC decreases by a factor of about 2 at high ionic strengths, while the crystalline body remains unchanged. This confirms the existence of soft, deformable regions on this nanoparticle, i.e., protruding dicarboxylated cellulose chains (DCC). A similar contraction is observed for SNCC when adding propanol (a poor solvent for dialdehyde cellulose).[54] (ii) The maximum theoretical surface charge of cellulose nanocrystals with a 10 nm × 10 nm crystal packing bearing glucose units (0.5 nm × 0.5 nm × 0.15 nm) is ≈ 0.8 meq g^{-1};[66] The charge density of ENCC is almost ten times as large, which attests to the presence of highly charged non-crystalline cellulose. (iii) When ENCC is hydrolyzed with a strong acid

(e.g., HCl), the charge content can be decreased by a factor of 10 without changing the crystal structure.[75] This is the result of cleaving highly charged amorphous chains (DCC). Our XRD experiments[75] show that by hydrolyzing ENCC with HCl (3 N) for 3 h, the crystallinity increases from 90% to 96 % while the surface charge decreases from 6.6 meq g^{-1} to 1.7 meq g^{-1} and the hydrodynamic size decreases from 230 nm to 135 nm, whereas the size of the crystalline body, obtained by TEM imaging, does not change. This proofs that during hydrolysis, the amorphous chains are severely reduced in size.

Evidence that chains are protruding from both ends

(i) When divalent cations, e.g., Cu(II), are introduced to an ENCC dispersion, star-like aggregates are formed[71] in which rod-like particles contact each other by their poles. The bridging of ENCC from their poles is a sign of pole-pole interactions, which suggests that calcium ions bind to the carboxylated chains protruding from both ends and bridge chains from different particles. (ii) A bioconjugation reaction between hydrolyzed ENCC-NH2 and hydrolyzed ENCC results in an end-to-end attachment of ENCCs, providing a versatile bottom-up tool to build elongated nanostructures (AFM image, Fig. 14).[72] This proves that after hydrolysis, most of the remaining carboxyl groups are located at the poles of hydrolyzed ENCC. Note that before hydrolysis, these groups were located on the protruding ends.

Finally, the successive periodate-chlorite oxidation reactions, introduced in this work, along with the properties of products attest well to the model of cellulose fibers comprising alternating crystalline and amorphous regions. Note that TEM and AFM imaging are unable to capture the amorphous regions of HCNC, because of a poor contrast in the non-crystalline regions. Our current efforts encompass using sophisticated imaging techniques such as liquid-phase TEM and cryo-TEM, which may help image the hair. Moreover, our endeavor to decorate ENCC with amine-functionalized gold nanoparticles through bioconjugation reactions is ongoing; however, fast dynamics of gold nanoparticles (size < 5 nm) and colloidal aggregation are among the difficulties of this imaging strategy. These goals are still a subject of investigation in our lab.

Potential applications of hairy cellulose nanocrystalloids

Transparent films

Hairy nanocelluloses form highly transparent films when dried.[67] Such films are stronger and more flexible then films made from conventional NCC, which are brittle. Their superior properties are due to the protruding polymer chains, which can entangle, thus forming strong films. For ENCC, the film properties depend on the counterion of the carboxyl group. Films in the sodium form (Na^+ as counterion) are more transparent and stronger and have higher water contact angles than films in the H-form (H^+ as counterion). An example of a highly transparent ENCC film is shown in Fig. 17.[67] This unique property of films prepared from hairy cellulose nanocrystalloids may be advantageous in developing nanopapers for high security purposes, sensors and actuators, and paper-based microfluidic devices.

Fig. 17 Transparent film (nanopaper) prepared from drying ENCC.[67] Reprinted with permission from Yang et al.,[67] Copyright (2012) American Chemical Society.

Superhydrophobic films

To provide a surface with superhydrophobicity, surface roughness on the nanoscale (to increase the surface area, Wenzel model,[76] and/or trap air bubbles under the water drop, Cassie model[77]) and the presence of hydrophobic groups on the surface are essential.[78] Films of nanocellulose benefit from the nanoscale build surface features, since their constituents, nanocrystalloids, have diameters in the range 5-10 nm, which can self-assemble upon drying. Thus, by chemically modifying hairy nanocellulose, one would expect to obtain superhydrophobic films (i.e., films with water contact angles > 150°). One way to achieve this is to crosslink the hairy nanocellulose particles (ENCC or SNCC) with a diamine. In the case of ENCC films, this can be achieved simply by dipping the ENCC film into TCMS (trichloromethylsilane,[79,80]) and subsequent drying. This produces contact angles of 160°.[67] Dipping an ENCC film in an ADH/EDC solution also produces superhydrophobic films. ADH (adipic dihydrazide) is a crosslinker and EDC (1-etyl-3-[3-(dimethylaminopropyl)] carbodiimide) is an activator, which are both required for the bioconjugation reaction to proceed. The crosslinking reduces the transparency from about 90 to 75% (for wavelengths > 500 nm), but increases the strength (tensile strength is increased from 63 to 104 MPa).[67]

Security packaging

Dry hairy nanocellulose can be readily dispersed in water, i.e., the hydrogen bonding between the nanoparticles in the dry state is reversed by the electrosteric repulsion in the wet state. Films made of hairy nanocellulose can be used for security packaging, e.g., packaging, which disappears when immersed in water. This provides a unique opportunity to manufacture smart coating and packaging based on green nanomaterials.

Heavy metal ion scavengers

Hairy nanocellulose particles with anionic or cationic charge groups (ENCC or CNCC) are able to scavenge cations or anions in aqueous solutions, respectively. As an example, we have investigated the

scavenging of Cu^{2+} by ENCC. These nanoparticles bear charge densities exceeding 6 meq g^{-1}, whereas the charge densities of conventional NCC are about 0.2 meq g^{-1}. ENCC scavenges a stoichiometric amount of charge, so the higher the charge density of ENCC, the more ions can be adsorbed. Accordingly, it is possible to take up 0.2 g Cu^{2+} per gram of ENCC (Fig. 18).[71]

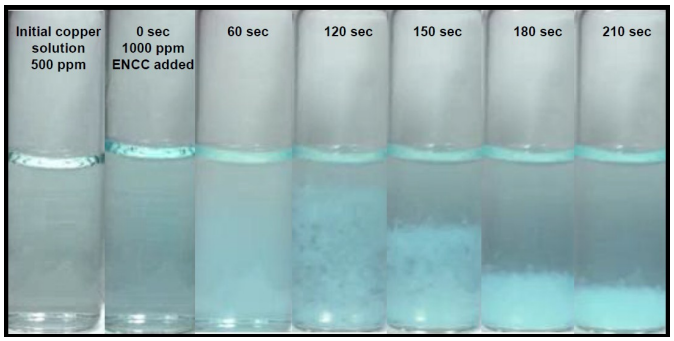

Fig. 18 Addition of ENCC to a copper solution results in the aggregation and precipitation of nanoparticles providing a facile way to remediate polluted aqueous media.[71] Reprinted with permission from Sheikhi et al.,[71] Copyright (2015) American Chemical Society.

At copper concentrations lower than the stoichiometric amount, initially (before the suspension is completely mixed), some of the ENCC are fully saturated while others are partially neutralized with copper ions. Reduced electrostatic force between the particles results in van der Waals-mediated aggregation to form nanosized star-like features (Fig. 19, left). Such self-assembly is of particular interest in designing separation processes in water treatment units. As the copper concentration increases, all the nanoparticles become saturated and form micron-sized raft-like aggregates (Fig. 19, right), which readily sediment. This provides a convenient and cost-effective method for separating the nanoadsorbent.[71] In principle, the heavy metal ions may be desorbed by decreasing pH or performing ion-exchange, and the ENCC particles can be used again. Furthermore, packed beds of ENCC, gel-loaded ENCC, and coated surfaces with ENCC are other alternatives for continuous heavy metal ion removal processes.

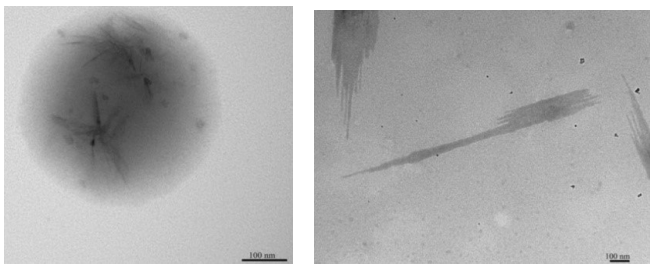

Fig. 19 Addition of Cu2+ to ENCC dispersion (1000 ppm) results in star-like (left) or raft-like (right) aggregation of nanocrystals at low (< 300 ppm) and high (> 300 ppm) copper concentrations, respectively. This provides a facile way to separate the nanoadsorbent from the treated water.[71] Reprinted with permission from Sheikhi et al.,[71] Copyright (2015) American Chemical Society.

Scavengers of non-ionic pollutants

One of the key parameters in removing non-ionic pollutants, such as dyes, is the polarity of the adsorbent.[81] Many organic pollutions can conceivably associate with DAMF chains, which benefit from a large aldehyde content. Thus, SNCC may act as a scavenger for such compounds. This warrants further investigation.

Cellulose hydrogels

Hydrogels are hydrophilic polymer networks, which can absorb water up to several orders of magnitude higher than their dry mass and swell.[82] Among the numerous applications of them are superabsorbents,[83] scaffolds and templates for tissue engineering,[84] and wound dressings.[85,86] Also, they can be used in food industry, e.g., in chocolate production[87]. Cellulose hydrogels made from hairy nanocelluloses are able to perform well for these functions owing to their high degree of functionality and reactivity. They benefit from these advantages to readily crosslink and form strong, biocompatible gels. An example of crosslinking ENCC with ADH was discussed previously to manufacture superhydrophobic surfaces; however, a wide range of crosslinkers with different properties may be used to produce HCNC-based hydrogels. For instance, we have synthesized in our lab a new family of sustainable hydrogels containing SNCC, which can take up water more than 3000 times its weight (to be submitted). It is also possible to produce gels that take up large quantities of oil by simply hydrophobizing the hydrogels.

Humidity switches

An interesting example which clearly shows the difference in conventional NCC and ENCC is their application in composites of carbon nanotubes (CNT) and nanocellulose. CNT-NCC composites conduct electricity, whereas CNT-ENCC composites are insulators when exposed to relative humidities below about 75%.[88] Above this, they become conductors, and thus, such composites can be used as humidity switches. An example of the electrical conductance of a CNT-ENCC composite (and a comparison with a CNT-NCC composite) is shown in Fig. 20. It can be seen that the electrical conductance of the CNT-ENCC composite, which is significantly low that it can be considered as an isolator, increases steeply at relative humidities greater than 75%.[88]

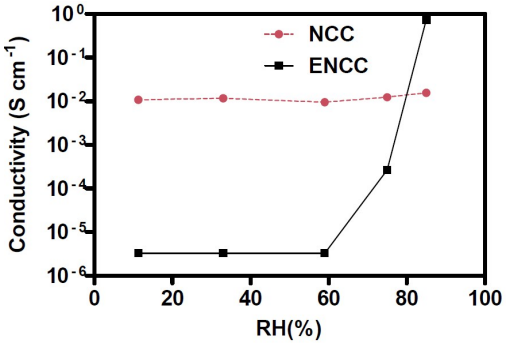

Fig. 20 Direct current conductivity of NCC and ENCC composites with 1 % carbon nanotube (CNT) content versus relative humidity (RH). At low RH, CNT-ENCC composites are insulators while at RH > 75%, they are conductors.[88] Reprinted with permission from Safari et al.,[88] Copyright (2016) American Chemical Society.

Polymer reinforcement

Within the past few years, cellulose-based nanocomposites have been able to play such an important role in an extraordinarily wide range of applications that imagining the world without them is implausible.[41] A key ingredient to produce such composites is nanocrystalline cellulose. Polymer-NCC composites have exhibited excellent mechanical performance owing to the reinforcement secured by the dispersed NCC[89] with a Young's modulus *O*(100 GPa[23]). Besides the physical effect of their stiff backbone, surface functionalization may enhance the NCC incorporation into the matrix. Hairy NCC provides high densities of functional groups ready to be further functionalized simply through water-based reactions (such as click chemistry) to engineer the surface properties for better dispersion and/or integration in the polymer matrix. Accordingly, they can be readily made compatible with the polymer of choice, because the protruding chains can be easily chemically modified.

Rheology modifiers

Owing to their small size and unique surface properties (OH and SO_3^- functional groups), nanocrystalline celluloses are able to form micro- and nanostructures with fluids when the interactions are favourable, thus modifying their rheological properties. An example of this application is nanocomposite drilling fluids, such as NCC-bentonite-water.[90] To achieve a desired modification, molecular interaction between the nanocrystal and medium must be engineered. It is likely that hairy nanocellulose can perform better due to its dense surface functionalization. HCNC has the advantage that their chemical structure of the protruding chains can be optimized for specific applications. As an example, HCNCs can benefit from their high colloidal stability in a pre-polymerization solution and maintain the viscosity low while providing sufficient functionalization for further reaction during the process. We have been able to use HCNC to tune the rheological properties (elastic and loss moduli) of metal-based hydrogels several orders of magnitude (to be submitted). Furthermore, for applications such as anti-icing agents, similar to NCC,[91] HCNC may be used as a thickening agent.

Flocculants

Polymer-mediated flocculation and bridging is of particular industrial interest.[92] Conventional NCC is often grafted with various polymers to bind to colloids and flocculate them; however, such polymer chains are readily available on HCNC. Hairy nanocelluloses can perform as bridging agents for the flocculation of colloids. We have shown that both SNCC and ENCC can flocculate calcium carbonate particles (PCC, precipitated calcium carbonate).[93] As (pure) $CaCO_3$ particles are positively charged, ENCC, which bears carboxylic acid groups, acts as a charge neutralizer, with the most accelerated flocculation occurring at the isoelectric point. SNCC also behaves as a bridging agent, owing to the protruding DAMC chains adsorbing on $CaCO_3$ (chains from each end adsorbing on a different particle). SNCC particles with the longest chains are the best bridging agents. CNCC can also act as a bridging agent only when most of the $CaCO_3$ surface is coated with a stabilizer or impurity providing negative surface charge. In this case, one end of CNCC can adsorb, leaving the other free end to adsorb on another negatively charged particle. It is likely that ENCC (CNCC) can flocculate most or all positively (negatively) stabilized colloids, whereas SNCC flocculates colloids with a high affinity for DAMC. These properties of HCNC qualify them as green additives for water treatment. Furthermore, such flocculants may be used as retention agents and play a key role in several industries such as papermaking by increasing the dewatering efficiency and lowering the cost of this rather expensive step.

Directed metal nanoparticle synthesis

Metal nanoparticles have gained a tremendous importance in a wide range of industrial, e.g., construction,[94] and biological, e.g., detection,[95] applications. Nevertheless, besides the surface functionality, their optical,[80] biological,[81] and catalytic[96] performance relies on the shape and crystal packing. We have shown that the grafting density of DCC chains on ENCC can be altered by controlled acid hydrolysis.[66] This has enabled us to modify the crystallization pathway of silver ions and gain facile control over the shape of silver nanoparticles. When the carboxylic acid content of ENCC is high (≈ 6.5 mmol g^{-1}), silver ions are regulated towards the formation of randomly-branched flower-like nanoparticles, while decreasing the charge content to ≈ 1.7 mmol g^{-1} resulted in the synthesis of well-defined triangular silver nanoprisms.[97] In fact, decreased charge content was achieved by decreasing the DCC chain size (cleaving through acid hydrolysis), which may result in less conformational freedom (randomness) of these chains. This may result in charge-dependent capping effect of ENCC by various mechanisms such as coincidence between the DCC and Ag crystal seed facets and/or matching between the DCC and Ag lattice constant, similar to the more favourable[98] interaction between citrate and Ag{111} than Ag{100}.

Biomimetic mineralization

Controlling the shape and crystal packing of inorganic precipitates plays a vital role in designing new reinforcing materials. In nature, some animals such as sea shells, snails, and coral reefs (ascidians) secrete an inorganic substance (e.g., calcium carbonate) in the presence of an inorganic material (e.g., protein). This process, commonly referred to as biomineralization,[99,100] allows animals to produce their desired morphology and (often thermodynamically unstable) crystal habit. Our experiments suggest that HCNC with proper functionalization (to be submitted) is able to stabilize early stages of calcium carbonate, i.e., amorphous calcium carbonate (ACC) and vaterite. This could not be achieved using NCC due to low surface group density.

Applications of DAMC, DCC and QAMC

The yield of hairy nanocellulose production (from cellulose fibers) is typically around 50%; therefore, it is essential to seek applications of the cellulose derivatives (non-crystalline biopolymers), which end up in the solution. This will greatly enhance the commercial feasibility of

producing hairy nanocelluloses for commercial applications. Here we point to a few potential applications.

Flocculants and stabilizers

Protruding DCC chains (from ENCC), DAMC chains (from SNCC), and QAMC chains (from CNCC) may adsorb on $CaCO_3$, depending on the calcium carbonate surface potential. Thus, DCC, DAMC, and QAMC should be able to flocculate $CaCO_3$ as well. As a proof of concept, we have shown that DCC can flocculate $CaCO_3$.[93,101] Similar to the ENCC, this biopolymer functions by charge neutralization with maximum flocculation occurring at the isoelectric point (zero surface potential). Interestingly, excess DCC coats the positively-charged colloidal particles, acting as a stabilizer. Similarly, DAMC can perform as either a flocculant (e.g., for $CaCO_3$) or a stabilizer, depending on the dosage. Fundamentally, partial coverage leads to flocculation and full coverage to steric stabilization. QAMC is likely to perform similar to DCC, as a flocculant or a stabilizer for negatively charged colloids.

Superabsorbent polymers

Hairy nanocelluloses can be readily made into superabsorbent polymers (SAP). Classical superabsorbent polymers consist of crosslinked polyacrylic acid,[102] derived from non-renewable resources (fossil fuels). Any crosslinked highly charged polymer (polyelectrolyte) can act as a SAP. DCC, as a by-product of ENCC, can have charge densities exceeding 6 meq g^{-1} (DS = 1), comparable to classical SAP. Thus, crosslinking DCC should result in SAP rivalling classical ones. It is also possible to crosslink SNCC (with a diamine) and subsequently to transform the remaining aldehyde groups into carboxyl groups by a chlorite oxidation. One can also crosslink SNCC with a crosslinker that links hydroxyl groups, such as epichlorohydrin (ECH) in a basic medium. Such chemistry has been widely used for crosslinking starch,[103] chitosan,[104] and cellulose.[105] QAMC is usually less charged than DCC, because it is difficult to attach a quaternary ammonium group on an aldehyde neighboring a reacted aldehyde, and, when crosslinked, is not expected to be an effective SAP. However, it might be possible to increase the number of charges.

Antiscalants

The formation of sparingly soluble salts, such as carbonates and silicates, referred to as scaling, is a serious issue of water-based industrial processes.[106] Most of the industrial scale inhibitors are phosphonated or nitrogen-based macromolecules, which poses a serious risk to ecosystems by accelerating the so-called eutrophication process.[106] Carboxylated celluloses, such as DCC, may be green replacements for synthetic antiscalants.[107–109]

Rheology modifiers

HCNCs bear a backbone (nanocrystalline cellulose) with an elastic modulus in the order of 100 GPa. This limits their applications at high concentrations. The biopolymeric counterparts of HCNC (DAMC, DCC, and QAMC) can provide similar functional groups to modify rheology while eliminating the crystalline body. This will enhance their usage at high concentrations with minor mechanical effect.

Specialty polymers

Special applications of polymers include but not limited to providing temperature resistivity and fire retardation[110,111] (e.g., clay nanopapers[112]), conduction (conductive textiles[113]), anti-icing properties (acrylic polymer blends[114]), ferroelectricity,[115] templates and supports,[116] drug carriers (chitosan[117]), and smart composites (tissue regeneration[118]). Renewability, abundance, ease of functionalizability in environmentally-friendly solvents, facile separation techniques, and large surface group density position DCC, DAMC, and QAMC for the next-generation specialty polymers.

Cytotoxicity of HCNC

Hairy nanocrystalline celluloses are able to provide a reliable infrastructure for drug[119] and marker[120] conjugation. Conventional nanocrystalline cellulose (concentration up to 50 ppm, exposure time 48 h) has shown no toxicity to various cell lines.[121] While being biologically safe, NCC suffers from low colloidal stability at high ionic strength media (e.g., physiological conditions).[70] HCNC overcomes this shortcoming owing to a high surface functionality and the excluded volume of attached biopolymers (steric repulsion). Moreover, a large surface group density permits partial functionalization of HCNC with drugs and biomarkers while maintaining the colloidal stability.[75] Despite these advantages, ENCC with carboxylic acid content more than ≈ 4 mmol g^{-1} has a negative effect on the mitochondrial activity of cells.[75] This does not seem to limit the application of HENCC as a new generation of drug and gene carrier, because their charge content can be easily modified.

Conclusions

Nanotechnology today is moving rapidly towards benefiting from environmentally-friendly materials to eliminate the adverse effects of synthetic nanomaterials. Among the recent advances in this era, functional nanoparticles from natural sources, e.g., cellulose-based micro- and nano-crystals, have been able to compete noticeably with synthetic nanomaterials, providing unique advantages such as biorenewability, biodegradability, cost efficiency, abundance, and ease of processing. One of the most promising candidates for such materials is nanocrystalline cellulose (NCC), which has been able to secure key roles in a significant array of advanced applications. This paper reviews the emergence of a new class of NCC bearing both crystalline and amorphous regions, referred to as hairy cellulose nanocrystalloids (HCNC). The unique surface properties, purely-chemical synthesis procedure, and high colloidal stability provide these nanoparticles with strikingly different physicochemical properties, which qualify them for a wider range of applications than conventional NCCs. Furthermore, the synthesis of HCNC involves the production of functional biopolymers, which indeed benefit from similar functionalities as HCNC, yet missing the crystalline part. This work provides a comprehensive study

on the current trends in designing new cellulose nanocrystals with emphasis on their applications, and sheds light on the potential role of HCNC as a key building block for facile, flexible, and reliable green nanotechnology.

Acknowledgements

Financial support from Natural Sciences and Engineering Research Council (Canada), Fonds de Recherche du Québec-Nature et technologies (FRQNT, Quebec, Canada), and Centre for Self-Assembled Chemical Structures (CSACS) is gratefully acknowledged.

Notes and references

1 N. Lin, J. Huang and A. Dufresne, *Nanoscale*, 2012, **4**, 3274.
2 T. Zimmermann, N. Bordeanu and E. Strub, *Carbohydr. Polym.*, 2010, **79**, 1086–1093.
3 M. Ioelovich, *BioResources*, 2008, **3**, 1403–1418.
4 M. A. Hubbe, O. J. Rojas, L. A. Lucia and M. Sain, *BioResources*, 2008, **3**, 929–980.
5 F. P. La Mantia and M. Morreale, *Compos. Part A Appl. Sci. Manuf.*, 2011, **42**, 579–588.
6 M. A. S. Azizi Samir, F. Alloin, A. Dufresne and M. A. S. A. Samir, *Biomacromolecules*, 2005, **6**, 612–626.
7 N. Lin and A. Dufresne, *Eur. Polym. J.*, 2014, **59**, 302–325.
8 M. Galotto and P. Ulloa, *Packag. Technol. Sci.*, 2010, **23**, 253–266.
9 A. Khan, T. Huq, R. a. Khan, B. Riedl and M. Lacroix, *Crit. Rev. Food Sci. Nutr.*, 2012, **8398**, 120904065059008.
10 Z. Wang, P. Tammela, P. Zhang, J. Huo, F. Ericson, M. Strømme and L. Nyholm, *Nanoscale*, 2014, **6**, 13068–75.
11 Z. Wang, P. Tammela, M. Strømme and L. Nyholm, *Nanoscale*, 2015, **7**, 3418–3423.
12 M. M. Hamedi, A. Hajian, A. B. Fall, K. Hkansson, M. Salajkova, F. Lundell, L. Wgberg and L. a. Berglund, *ACS Nano*, 2014, **8**, 2467–2476.
13 L. Hu, G. Zheng, J. Yao, N. Liu, B. Weil, M. Eskilsson, E. Karabulut, Z. Ruan, S. Fan, J. T. Bloking, M. D. McGehee, L. Wågberg and Y. Cui, *Energy Environ. Sci.*, 2013, **6**, 513–518.
14 H. Koga, T. Saito, T. Kitaoka, M. Nogi, K. Suganuma and A. Isogai, *Biomacromolecules*, 2013, **14**, 1160–1165.
15 M. Nogi and H. Yano, *Adv. Mater.*, 2008, **20**, 1849–1852.
16 G. Zheng, Y. Cui, E. Karabulut, L. Wågberg, H. Zhu and L. Hu, *MRS Bull.*, 2013, **38**, 320–325.
17 Z. Shi, G. O. Phillips and G. Yang, *Nanoscale*, 2013, **5**, 3194.
18 C. Yan, J. Wang, W. Kang, M. Cui, X. Wang, C. Y. Foo, K. J. Chee and P. S. Lee, *Adv. Mater.*, 2014, **26**, 2022–2027.
19 H. Golmohammadi, T. Naghdi, H. Yousefi, U. Kostiv, E. Morales-narva and D. Hora, 2015, 7296–7305.
20 A. W. Martinez, S. T. Phillips, G. M. Whitesides and E. Carrilho, *Anal. Chem.*, 2010, **82**, 3–10.
21 G. Siqueira, J. Bras and A. Dufresne, *Polymers.*, 2010, **2**, 728–765.
22 K. Torvinen, J. Sievanen, T. Hjelt and E. Hellen, *Cellulose*, 2012, **19**, 821–829.
23 A. Dufresne, *Mater. Today*, 2013, **16**, 220–227.
24 D. J. Gardner, G. S. Oporto, R. Mills and M. A. S. A. Samir, *J. Adhes. Sci. Technol.*, 2008, **22**, 545–567.
25 S. Rebouillat and F. Pla, *J. Biomater. Nanobiotechnol.*, 2013, **04**, 165–188.
26 TAPPI, *International nanocellulose standards: The need and purpose of standards for nanocellulosic materials*, GA, 2011.
27 D. Klemm, F. Kramer, S. Moritz, T. Lindström, M. Ankerfors, D. Gray and A. Dorris, *Angew. Chem. Int. Ed.*, 2011, **50**, 5438–5466.
28 C. J. Chirayil, L. Mathew and S. Thomas, *Rev. Adv. Mater. Sci.*, 2014, **37**, 20–28.
29 D. Klemm, D. Schumann, F. Kramer, N. Heßler, M. Hornung, H. P. Schmauder and S. Marsch, *Adv. Polym. Sci.*, 2006, **205**, 49–96.
30 D. Le Corre, J. Bras and A. Dufresne, *Biomacromolecules*, 2010, **11**, 1139–1153.
31 N. R. Savadekar and S. T. Mhaske, *Carbohydr. Polym.*, 2012, **89**, 146–151.
32 R. J. Moon, A. Martini, J. Nairn, J. Simonsen and J. Youngblood, *Cellulose nanomaterials review: structure, properties and nanocomposites.*, 2011, vol. 40.
33 H. P. S. Abdul Khalil, Y. Davoudpour, M. N. Islam, A. Mustapha, K. Sudesh, R. Dungani and M. Jawaid, *Carbohydr. Polym.*, 2014, **99**, 649–665.
34 K. Missoum, M. Belgacem and J. Bras, *Materials (Basel).*, 2013, **6**, 1745–1766.
35 A. Isogai, T. Saito and H. Fukuzumi, *Nanoscale*, 2011, **3**, 71–85.
36 T. Saito, Y. Nishiyama, J. L. Putaux, M. Vignon and A. Isogai, *Biomacromolecules*, 2006, **7**, 1687–1691.
37 T. Saito and A. Isogai, *Biomacromolecules*, 2004, **5**, 1983–1989.
38 T. Saito, M. Hirota, N. Tamura, S. Kimura, H. Fukuzumi, L. Heux and A. Isogai, *Biomacromolecules*, 2009, **10**, 1992–1996.
39 T. Isogai, T. Saito and A. Isogai, *Cellulose*, 2011, **18**, 421–431.
40 R. Shinoda, T. Saito, Y. Okita and A. Isogai, *Biomacromolecules*, 2012, **13**, 842–849.
41 S. J. Eichhorn, A. Dufresne, M. Aranguren, N. E. Marcovich, J. R. Capadona, S. J. Rowan, C. Weder, W. Thielemans, M. Roman, S. Renneckar, W. Gindl, S. Veigel, J. Keckes, H. Yano, K. Abe, M. Nogi, a. N. Nakagaito, A. Mangalam, J. Simonsen, a. S. Benight, A. Bismarck, L. a. Berglund and T. Peijs, *J. Mater. Sci.*, 2010, **45**, 1–33.
42 Y. Habibi, L. A. Lucia and O. J. Rojas, *Chem. Rev.*, 2010, **110**, 3479–3500.
43 Y. Habibi, H. Chanzy and M. R. Vignon, *Cellulose*, 2006, **13**, 679–687.
44 A. O'sullivan, *Cellulose*, 1997, **4**, 173–207.
45 Y. Habibi, L. A. Lucia and O. J. Rojas, 2010, **d**, 3479–3500.
46 J. F. Revol, H. Bradford, J. Giasson, R. H. Marchessault and D. G. Gray, *Int. J. Biol. Macromol.*, 1992, **14**, 170–172.
47 K. Conley, L. Godbout, M. a. (Tony) Whitehead and T. G. M. van de Ven, *Carbohydr. Polym.*, 2016, **135**, 285–299.

48 E. Maekawa and T. Koshijima, *J. Appl. Polym. Sci.*, 1984, **29**, 2289–2297.
49 R. D. Guthrie, *Adv Carbohydr Chem.*, 1961, **16**, 105–158.
50 E. L. Jackson and C. S. Hudson, *J. Am. Chem. Soc.*, 1937, **59**, 2049–2050.
51 L. Jackson and C. S. Hudson, 1938, **60**, 989–991.
52 A. Potthast, S. Schiehser, T. Rosenau and M. Kostic, *Holzforschung*, 2009, **63**, 12–17.
53 X. Liu, L. Wang, X. Song, H. Song, J. R. Zhao and S. Wang, *Carbohydr. Polym.*, 2012, **90**, 218–223.
54 H. Yang, D. Chen and T. G. M. van de Ven, *Cellulose.*, 2015, **22**, 1743–1752.
55 D. Chen and T. G. M. van de Ven, *Cellulose*, 2016.
56 J. T. Overbeek, *Progr. Biophys. Biophys. Chem.*, 1959, **6**, 58–84.
57 H. Liimatainen, J. Sirviö, H. Pajari, O. Hormi and J. Niinimäki, *J. Wood Chem. Technol.*, 2013, **33**, 258–266.
58 H. Yang and T. G. M. van de Ven, *Cellulose*, 2016, **In Press**, 1–11.
59 D. H. Napper, *J. Colloid Interface Sci.*, 1977, **58**, 390–407.
60 D. H. Napper, *Polymeric stabilization of colloidal dispersions*, Academic Press, London, 1984.
61 G. J. Fleer, M. A. Cohen Stuart, J. M. H. M. Scheutjens, T. Cosgrove and B. Vincent, *Polymers at interfaces*, Chapman and Hall, London, 1993.
62 U.S. Provisional Patent Application 3776923-v3, 2011.
63 H. A. Rutherford, F. W. Minor, A. R. Martin and M. Harris, *J. Res. Nat. Bur. Stand*, 1942.
64 B. . Hofreiter, I. a. Wolff and C. L. Mehltretter, *J. Am. Chem. Soc.*, 1957, **79**, 6457–6460.
65 M. Floor, J. A. Peters, H. van Bekkum, A. P. G. Kieboom, J. H. Koek, F. L. M. Smeets and R. E. Niemantsverdriet, *Carbohydr. Res.*, 1990, **203**, 19–32.
66 H. Yang, M. N. Alam and T. G. M. van de Ven, *Cellulose.*, 2013, **20**, 1865–1875.
67 H. Yang, A. Tejado, N. Alam, M. Antal and T. G. M. van de Ven, *Langmuir*, 2012, **28**, 7834–7842.
68 A. Sheikhi, H. Yang, M. N. Alam and T. G. M. van de Ven, *J. Vis. Exp*, 2016, **In Press**.
69 G. T. Hermanson, in *Bioconjugate Techniques (Third edition)*, 2013, pp. 229–258.
70 S. Safari, A. Sheikhi and T. G. M. van de Ven, *J. Colloid Interface Sci.*, 2014, **432**, 151–157.
71 A. Sheikhi, S. Safari, H. Yang and T. G. M. van de Ven, *ACS Appl. Mater. Interfaces.*, 2015, **7**, 11301–11308.
72 H. Yang and T. G. M. van de Ven, *Submitted*, 2016.
73 U. J. Kim, S. Kuga, M. Wada, T. Okano and T. Kondo, *Biomacromolecules.*, 2000, **1**, 488–492.
74 J. Araki, M. Wada and S. Kuga, *Cellulose.*, 2001, **17**, 21–27.
75 Z. Hosseinidoust, M. N. Alam, G. Sim, N. Tufenkji and T. G. M. Van De Ven, *Nanoscale*, 2015, **7**, 16647–16657.
76 R. N. Wenzel, *J. Ind. Eng. Chem.*, 1936, **28**, 988–994.
77 A. B. D. Cassie and S. Baxter, *Trans. Faraday Soc.*, 1944, 546–551.
78 A. Lafuma and D. Quéré, *Nat. Mater.*, 2003, **2**, 457–60.
79 A. Tejado, W. C. Chen, M. N. Alam and T. G. M. van de Ven, *Cellulose*, 2014, **21**, 1735–1743.
80 W. C. Chen, A. Tejado, M. N. Alam and T. G. M. van de Ven, *Cellulose*, 2015, **22**, 2749–2754.
81 G. Crini, *Bioresour. Technol.*, 2006, **97**, 1061–85.
82 C. Chang and L. Zhang, *Carbohydr. Polym.*, 2011, **84**, 40–53.
83 A. Sannino, C. Demitri and M. Madaghiele, *Materials (Basel).*, 2009, **2**, 353–373.
84 S. Van Vlierberghe, P. Dubruel and E. Schacht, *Biomacromolecules*, 2011, **12**, 1387–1408.
85 W. Czaja, A. Krystynowicz, S. Bielecki and R. M. Brown, *Biomaterials*, 2006, **27**, 145–151.
86 L. Fu, J. Zhang and G. Yang, *Carbohydr. Polym.*, 2013, **92**, 1432–1442.
87 Z. Shi, Y. Zhang, G. O. Phillips and G. Yang, *Food Hydrocoll.*, 2014, **35**, 539–545.
88 S. Safarimohsenabad and T. G. M. van de Ven, *ACS Appl. Mater. Interfaces*, 2016, **8**, 9483–9489.
89 C. Miao and W. Y. Hamad, *Cellulose*, 2013, **20**, 2221–2262.
90 M. C. Li, Q. Wu, K. Song, Y. Qing and Y. Wu, *ACS Appl. Mater. Interfaces*, 2015, **7**, 5009–5016.
91 European Patent Office, EP0257720 B1, 1990.
92 T. G. M. van de Ven and B. Alince, *J. Colloid Interface Sci.*, 1996, **181**, 73–78.
93 D. Chen, Ph.D. Thesis, McGill University, 2015.
94 J. Lee, S. Mahendra and P. Alvarez, *ACS Nano*, 2010, **4**, 3580–3590.
95 H. Jans and Q. Huo, *Chem. Soc. Rev.*, 2012, **41**, 2849.
96 R. Narayanan and M. A. El-Sayed, *Nano Lett.*, 2004, **4**, 1343–1348.
97 Z. Hosseinidoust, T. G. M. van de Ven and N. Tufenkji, *Submitted*, 2016.
98 J. Zeng, Y. Zheng, M. Rycenga, J. Tao, Z. Y. Li, Q. Zhang, Y. Zhu and Y. Xia, *J. Am. Chem. Soc.*, 2010, **132**, 8552–8553.
99 S. Weiner and L. Addadi, *Annu. Rev. Mater. Res.*, 2011, **41**, 21–40.
100 F. C. Meldrum, *Int. Mater. Rev.*, 2003, **48**, 187–224.
101 D. Chen and T. G. M. van de ven, *Submitted*, 2016.
102 M. J. Zohuriaan-Mehr and K. Kabiri, *Iran. Polym. J.*, 2008, **17**, 451–477.
103 L. Kuniak and R. H. Marchessault, *Starch - Stärke*, 1972, **24**, 110–116.
104 S. H. Lee, S. Y. Park and J. H. Choi, *J. Appl. Polym. Sci.*, 2004, **92**, 2054–2062.
105 Y. X. Bai and Y. F. Li, *Carbohydr. Polym.*, 2006, **64**, 402–407.
106 A. Sheikhi, N. Li, T. G. M. van de Ven and A. Kakkar, *Environ. Sci. Water Res. Technol.*, 2016, **2**, 71–84.
107 M. Chaussemier, E. Pourmohtasham, D. Gelus, N. Pécoul, H. Perrot, J. Lédion, H. Cheap-Charpentier and O. Horner, *Desalination*, 2015, **356**, 47–55.
108 D. Hasson, H. Shemer and A. Sher, *Ind. Eng. Chem. Res.*, 2011, **50**, 7601–7607.
109 US Patent, 4,561,982, 1985.
110 R.W. Dyson, *Specialty polymers*, 1987.
111 A. R. Horrocks, *Polym. Degrad. Stab.*, 1996, **54**, 143–154.
112 A. Liu, A. Walther, O. Ikkala, L. Belova and L. A. Berglund, *Biomacromolecules*, 2011, **12**, 633–641.
113 L. Dall'Acqua, C. Tonin, R. Peila, F. Ferrero and M. Catellani, *Synth. Met.*, 2004, **146**, 213–221.

114 L. Cao, A. K. Jones, V. K. Sikka, J. Wu and D. Gao, *Langmuir*, 2009, **25**, 12444–12448.
115 H. S. Nalwa, *Ferroelectric Polymers: Chemistry: Physics, and Applications*, CRC Press, 1995.
116 D. Belluš, *J. Macromol. Sci. Part A*, 1994, **31**, 1355–1376.
117 W. Paul and C. P. Sharma, *S.T.P. Pharma Sci.*, 2000, **10**, 5–22.
118 R. A. Perez, J. E. Won, J. C. Knowles and H. W. Kim, *Adv. Drug Deliv. Rev.*, 2013, **65**, 471–496.
119 J. K. Jackson, K. Letchford, B. Z. Wasserman, L. Ye, W. Y. Hamad and H. M. Burt, *Int. J. Nanomedicine*, 2011, **6**, 321–330.
120 S. Dong and M. Roman, *J. Am. Chem. Soc.*, 2007, **129**, 13810–13811.
121 S. Dong, A. A. Hirani, K. R. Colacino, Y. W. O. O. Lee and M. Roman, *Nano Life*, 2012, **02**, 1241006.